Open Veterinary Journal, (2024), Vol. 14(1): 304–315
ISSN: 2226-4485 (Print)
ISSN: 2218-6050 (Online)
Original Research
DOI: *10.5455/OVJ.2024.v14.i1.27*

Submitted: 01/10/2023 Accepted: 15/12/2023 Published: 31/01/2024

Ameliorative effect of *Odontonema cuspidatum* extract against testicular damage induced by sodium nitrite in rats

Nesma H. Elsawy[1*], Samir A. Elshazly[1], Azza M. Elkattawy[1], Nasr E. Nasr[1], Essam A. Almadaly[2], Mohamed S. Refaey[3], Khaled A. Kahilo[1], Mona Assas[4], Walied Abdo[5], Aml S. hashem[6], Tarek K. Abouzed[1] and Doaa Abdullah Dorghamm[1]

[1]*Department of Biochemistry, Faculty of Veterinary Medicine, Kafrelsheikh University, Kafrelsheikh, Egypt*
[2]*Department of Theriogenology, Faculty of Veterinary Medicine, Kafrelsheikh University, Kafrelsheikh, Egypt*
[3]*Department of Chemistry, Faculty of Science, Menoufia University, Shebin El-Koom, Egypt*
[4]*Fish Processing and Biotechnology Department, Faculty of Aquatic and Fisheries Sciences, Kafrelsheikh University, Kafrelsheikh, Egypt*
[5]*Department of Veterinary Pathology, Faculty of Veterinary Medicine, Kafrelsheikh University, Kafrelsheikh, Egypt*
[6]*Department of Biochemistry, Faculty of Veterinary Medicine, Alexandria University, Alexandria, Egypt*

ABSTRACT

Background: Sodium nitrite ($NaNO_2$) is a chemical substance used to enhance taste, add color, and keep food products fit for consumption for a longer time. $NaNO_2$ gives rise to a negative adverse effect on male reproductive function. *Odontonema cuspidatum* (OC) is a natural plant that possesses antioxidant capacity.

Aim: Our research evaluates the potential beneficial effect of OC extract on the harmful effects caused by $NaNO_2$ on the testicular tissue and sperm characteristics of male rats.

Methods: Four groups with a total of forty rats: the control, the $NaNO_2$-received group, the OC-administered group, and the fourth group received both $NaNO_2$ and OC. All groups were administered daily for two months. Sperm characteristics, testicular antioxidant status, qRT-PCR, and histopathological changes were evaluated.

Results: Coadministration of $NaNO_2$ and OC, in comparison with $NaNO_2$ alone, contributed to a notable enhancement in acrosomal integrity, decreasing sperm abnormalities and restoring serum testosterone levels. Moreover, such coadministration reduced the oxidative stress marker, malondialdehyde (MDA), and increased superoxide dismutase (SOD) in testicular tissue, lowering TNF-α gene expression, and increasing the expression of P450scc and StAR genes. In addition, the $NaNO_2$ and OC combination decreased the testicular histopathological changes and the Caspase-3 and Proliferating cell nuclear antigen (PCNA) immunoexpression in seminiferous tubules compared with the $NaNO_2$ group.

Conclusion: The extract of OC exhibited the ability to decrease oxidative stress and ameliorate the detrimental effects caused by $NaNO_2$.

Keywords: $NaNO_2$, *Odontonema cuspidatum*, Food additives, Testicular damage.

Introduction

Food additives include coloring agents, flavoring agents, emulsifiers, stabilizers, and preservatives that can be either natural or synthetic (Khodjaeva *et al*., 2013). Currently, manufactured food additives have progressively overtaken natural food additives, and there are numerous harmful effects of food additives, such as the abuse of chemicals, their overuse, or even their toxicity.

Food additives undoubtedly provide consumers with a lot of flavor satisfaction; however, they could additionally pose health hazards to humans. Therefore, it is extremely important to limit the consumption of food additives (Wu *et al*., 2022).

$NaNO_2$ is a widely used food additive found in various processed meat as well as fish products (JørgenandMarianne, 2011). It is generally known that $NaNO_2$ is frequently employed in additives to enhance taste and add color (Wang *et al*., 2022).

In addition, various medical processes can be controlled through $NaNO_2$ (Deng, 2006). It has therapeutic uses for medical problems such as heart attack and bleeding stroke (Pluta *et al*., 2005). Earlier studies have shown that sodium nitrite ($NaNO_2$) prevents the presence of dangerous bacteria, particularly spores of *Clostridium botulinum* (Difonzo *et al*., 2022). Conversely, receiving too much $NaNO_2$ has a harmful effect by generating free radicals, which upset the equilibrium between oxidants

***Corresponding Author:** Nesma Hussein Elsawy. Department of Biochemistry, Faculty of Veterinary Medicine, Kafrelsheikh University, Kafrelsheikh, Egypt. Email: *Nesma.Alsawy_a009@vet.kfs.edu.eg*

and antioxidants and have deleterious biological effects (Jensen, 2007; Naik *et al*., 2006).

The uncontrolled use of $NaNO_2$ has been implicated in several adverse health effects (Ansari *et al*., 2017). Notably, excess $NaNO_2$ disrupts reproductive hormones (Pavlova *et al*., 2017), and raises inflammatory cytokines in the testis (Alyoussef and Al-Gayyar, 2016).

This prompted our investigation into the impact of $NaNO_2$ on rat spermatogenesis. The incidence of cancer in adults has been linked to $NaNO_2$ exposure, and the occurrence of childhood nasopharyngeal cancers, blood cancer, and neurological tumors has also been linked to it (Kozisek, 2007).

Recent years have seen a rise in popularity and widespread acceptance of the use of herbal medicines in the treatment of numerous disorders and dysfunctions (Oyagbemi and Odetola, 2010). The use of herbal remedies to treat illnesses has persisted for many generations (Chaughule and Barve, 2023). They are popular due to their low cost, cultural acceptance, and lack of drawbacks (Chaughule and Barve, 2023).

One of these herbal plants is *Odontonema cuspidatum* (OC), which belongs to the Acanthaceae family. Its leaf extract contains flavonoids, saponins, glycosides, tannins, steroids, and terpenoids (Pierre and Moses, 2015), so it has antioxidant activity against lipid peroxidation due to their high flavonoid content (Refaey *et al*., 2015).

Our research evaluates the potential beneficial impact of OC extract against testicular damage induced by $NaNO_2$.

Materials and Methods

Chemicals

$NaNO_2$ was obtained from Merck KGaA (Darmstadt, Germany), with a purity of 96% (CAT NO. 7632-00-0). Absolute ethanol was purchased from Merck KGaA (Darmstadt, Germany). The formaldehyde solution was provided by PIOCHEM Co (Giza, Egypt), and chloroform was purchased from Fisher Scientific UK Ltd. (Leicestershire, UK). Glutaraldehyde (25% aqueous solution) was obtained from Oxford Lab Chem Maharashtra, India. The real-time SYBR Green Master Mix acquired by Applied Biotechnology Co. Macrogen Company (Korea) produced the PCR primers; the Primers 3 Program was used to build these sequences. Phosphate buffer (PBS) was purchased from Schwabach, Germany.

Kits

Serum sex hormones were assayed by the enzyme-linked immunosorbent assay (ELISA). Testosterone kits (Catalogue No. 201-11-5126), follicle-stimulating hormone (FSH) kits (Catalogue No. 201-11-0183), and luteinizing hormone (LH) kits were acquired from Sun Red Biotechnology Company, (Shanghai, China) (Catalogue No. 201-11-2119). Kits of malondialdehyde (MDA) (MD 25 29) and SOD (SD 25 21) were obtained from Biodiagnostics Company, (Cairo, Egypt). Enzynomics (Daejeon, Republic of Korea) provided the cDNA synthesis kit. Macrogen (Seoul, Republic of Korea) performed the synthesis of primers for β-actin, TNF-α, StAR, and p450scc.QIAGEN Company., (Maryland, USA) supplied the Qiazol lysis reagent. LobaChemie (Mumbai, India) provided the PBS.

Plant material

In October 2021, fresh aerial parts of OC were gathered from a private garden in Menoufia, Egypt. Therese Labib, the El Orman head (Botanical Garden), verified the plant material of *O. cuspidatum.*

Extraction procedure

To obtain the extract, methanol was macerated with 250 g of freshly powdered dried *O. cuspidatum's* aerial portions at room temperature until complete exhaustion (1 l × 3). Afterward, low pressure was used to concentrate the methanolic extract at 40℃, the resulting yellowish–green viscous residues weighed 302 g. The methanolic extract was then dried and preserved at 4°C for use in *in vivo studies*.

Animals

The Animal House at the Veterinary Medicine Faculty, University of Kafr Elsheikh (Egypt) provided 40 adult male Wistar albino rats weighing between 120 and 140 g. These rats were housed in adequately ventilated metal cages with wood shavings bedding under regular hygienic conditions. They were provided with water *ad libitum* and a basal diet from Dakahlia Company, Egypt. Animals were exposed to a cycle of light and dark with a duration of 12 hours each and maintained at 20°C–25°C. Before starting the experiment, the animals were given two weeks to adapt to their new environment.

Design of the experiment

Four groups with a total of forty rats, every group consisted of 10 rats. All groups were given their respective doses orally via gastric tubes daily for 2 months. Control: This group received only half a milliliter of distilled H_2O (DW). $NaNO_2$: They were orally given 80 mg/kg of $NaNO_2$ soluble in DW (Akhzari *et al*., 2019).

OC: They were given 100 mg of OC extract dissolved in a 1% carboxymethylcellulose solution (Kasali *et al*., 2022).

$NaNO_2$ + OC: They simultaneously received 80 mg/kg $NaNO_2$ and 100 mg/kg OC extract.

Blood sampling

The rats were administered intramuscular anesthesia using xylazine (10 mg/kg) with ketamine (125 mg/kg) in a combination (Veilleux-Lemieux *et al*., 2013). Heparinized capillary tubes were used to collect blood from the eye's medial canthus. We allowed the blood to coagulate, then centrifuged for 10 minutes at 3,500 rpm, collected serum, transferred it into Eppendorf tubes, then remained at −20°C up till measurement of the sex hormones.

Tissue sampling and homogenization

For euthanasia, the rats were decapitated, their testes and epididymis were taken, and the right testis was

preserved for histopathological investigation in a 10% neutral buffered formalin solution. The left testis was divided into three parts. One part, together with the adjacent epididymis, was used to assess sperm parameters. The second part was rapidly frozen at −80°C to extract RNA for gene expression examination related to testicular function, whereas the third portion was preserved at −20°C to determine oxidative stress markers, 10% homogenate was prepared by adding 0.01 M PBS with pH 7.4, to this portion. Then, the mixture was subjected to homogenization at 12,000 rpm on ice. After homogenization, the tissue's homogenate was centrifuged at 3,000 rpm for ten minutes at 4°C.

Assessment of body weight and testicular weight

Each rat's final body weight in each group was measured. In addition, the testes of the rats were removed and weighed after euthanasia by decapitation.

Assessment of gonadosomatic index (GSI)

GSI = (Mean weight of the combined testes/Final body weight) x 100 (Mostafa-Hedeab *et al*., 2023).

Sperm characteristics

For the examination of sperm characteristics, the rats were euthanized by decapitation. A sterile scalpel blade was used to make a mid-caudoventral abdominal incision for post-mortem examination. Immediately after euthanasia, the testes were dissected and weighed along with the epididymis using a sensitive electronic weighing machine. The testes and epididymis were then sliced to collect sperm cells in freshly prepared warm 2.9% sodium citrate dihydrate solution.

Sperm motility

Sperm motility was evaluated using the method described (Aly and Azhar, 2013). A small amount of sperm mixture was put on a warm glass slide, and a cover slip measuring 18 × 18 mm was placed over it. The slide was examined using phase-contrast (400×) microscopy. The motility included two types: progressive (movement in straight lines or large circles) and total motility (all forms of sperm movement, including straight, circular, and oscillatory).

Plasma membrane integrity

The HOS-test assay was performed. This involved mixing the sperm mixture (100 µl) and hypoosmotic solution (1,000 µl) warmed to the appropriate temperature. To make the hypoosmotic solution, sodium citrate dihydrate (7.35 g) and fructose (1.351 g) were dissolved in 100 ml of DW, resulting in an osmolarity of 150 mOsm/L. Then, the sperm mixture was placed in an incubator at 37°C for 45 min. Subsequently, the sperm suspension (2 µl) was added to a glass slide with a cover slip. To view these slides, we utilized phase-contrast microscopy with a magnification power of 400×. The sperms showing swollen or curled tails were considered intact, while those lacking this feature were considered damaged. To ensure accurate results, any sperm cells exhibiting tail abnormalities were carefully identified to obtain precise HOS test-positive spermatozoa (Almadaly *et al*., 2016).

Acrosomal integrity

The retrieved sperm cells were fixed using a solution containing 2% Glutaraldehyde in Sodium Cacodylate buffer with a pH of 7.3 (Almadaly *et al*., 2012). Fifty microliters of Glutaraldehyde were mixed with 50 µl of the sperm suspension, followed by an incubation period of 30–60 minutes. After incubation, phase-contrast microscopy was utilized to examine a drop of 2 µl of the sperm suspension at a magnification power of 100×. Sperm cells showing a consistent and uniform apical edge were considered to have intact acrosomes, while those with a muffled or uneven apical edge were classified as having damaged acrosomes.

Sperm viability and morphology

The eosin–nigrosin stain evaluated the spermatozoa's viability and morphology. After mixing an equal amount of sperm mixture and the dye, spread it onto a clean glass slide, and then allow it to dry on a warming plate. During the examination, sperm cells with unstained sperm heads were regarded as viable, while nonviable sperm showed the opposite (Talebi *et al*., 2007). Abnormal sperm cells were assayed using the stained smear under an oil immersion lens (Mortimer and Mortimer, 1992).

Assessment of testicular MDA level and SOD activity

Kits of MDA (MD 25 29) and SOD (SD 25 21) were obtained from Biodiagnostics Company (Cairo, Egypt). The colorimetric method is used to measure testicular MDA level and SOD activity according to Ohkawa *et al*. (1979) and Nishikimi (1975), respectively.

Hormonal analysis

Rat ELISA kits were used to measure Serum sex hormones, following their instructions. All hormonal kits were acquired from Sun Red Biotechnology Company (Shanghai, China).

Real-time polymerase chain reaction (RT-PCR)

RNA extraction

The testicular samples' total RNA was extracted in all experimental groups using the QIAzol reagent. After dissolving the extracted RNA pellet in RNase-free water, the extracted RNA's purity and concentration were estimated at absorbance at 260/280 nanometers by a NanoDrop 2000 spectrophotometer (Biochrom Ltd, Cambridge CB23 6DW, UK). The RNA's integrity and purity have been examined by running the samples on a 2% agarose gel and analyzing the resulting bands. Only RNA samples that met high-quality criteria, including an absorbance ratio of 260/280 in the range of 1.8 and 2.0.

cDNA synthesis

The RNA was reverse transcribed using the TOPScriptTM RT cDNA synthesis kit. According to their guidelines, mix total RNA (1 µg) with 10 µl of 2X RT reaction Solution and enzymes (1 µl), then add RNase-free water to the final volume of 20 µl. Incubation of these combinations for 30 minutes at 50°C, followed by 10 minutes at 85°C was preceded.

Quantitative real-time polymerase chain reaction (qRT-PCR)

The protocol of qRT-PCR included heating at 92°C for 10 min to denature the samples followed by amplification for 40 cycles, where the samples underwent annealing at 55°C and extension at 72°C. To detect relative gene expression, we utilized the 2−ΔΔCT technique, which involved normalizing the results to the expression levels of β-actin. Primers for the targeted genes are described in Table 1.

Histopathology

Ten percent neutral buffered formalin was used to fix the testicular tissue and underwent the following standard paraffin embedding procedures for tissue preparation. After fixation, the tissues were subjected to a process of dehydration using a series of ethyl alcohol concentrations that gradually increased. Then, tissues were cleared with xylene, subsequently embedded in paraffin wax, after that was sliced into sections of 5 µm thickness, and subsequently subjected to staining using the hematoxylin and eosin (H&E) stain (Bancroft *et al*., 2013). The light microscope **(**Leica DFC295) was used to examine the tissue sections to evaluate any histopathological alterations in the testes among all experimental groups. We used the well-reproducible criteria formed by Johnsen (1970). For quantifying spermatogenesis, the Johnsen criteria scored using a ten-point system, Johnsen scores vary from 1 to 10, with 1 referring to no germ cells and 10 referring to the highest spermatogenesis activity.

Immunohistochemistry

The immunohistochemical staining procedures are detailed in the study conducted (Khalil *et al*., 2020) which consisted of several sequential steps. The first step involved dewaxing the sections before their exposure to 0.05 M citrate buffer (pH 6.8), which was necessary for antigen retrieval. The next step involved treating the sections with protein block and 0.3% H_2O_2 to mitigate nonspecific binding. Afterward, the sections underwent incubation with anti-NF-κB P65 (Santa Cruz, Cat# (F-6): sc-8008), diluted 1/100, caspase 3 antibodies (Invitrogen, Cat# PA5-77887), diluted 1/100, in addition to PCNA Polyclonal rabbit Dako, USA, PA5-32541 at a dilution of 1/100. After rinsing the tissue sections with phosphate-buffered saline, they were exposed to a goat anti-rabbit secondary antibody (Cat# K4003, Envision+™ System Horseradish Peroxidase Labeled Polymer; Dako) for 30 minutes at ambient temperature to detect polyclonal antibodies. Next, we used Mayer's hematoxylin and the DAB kit to observe the sections. To represent the proportion of cells that exhibited positive results for the antibodies, staining labeling indices were determined out of 1,000 testicular spermatogenic cells.

Statistical analysis

Statistical analysis was done using GraphPad Prism version 9.5 (GraphPad Software Inc., San Diego, USA. The variance groups were identified by performing a one-way analysis of variance (ANOVA) and applying Tukey's test. $p < 0.05$ was employed to determine the level of statistical significance. To facilitate the interpretation and evaluation of the results, quantitative variables, such as the mean ± standard error of the mean (SEM), are employed for representation.

Ethical approval

The Institutional Animal Care and Use Committee's (IACUC) guidelines at the Veterinary Medicine Faculty, Kafr Elsheikh, Egypt, were followed with license number KFS-IACUC/134/2023.

Results

The weight of the body and testicles in addition to the gonad somatic index

The final body weight was significantly reduced ($p < 0.05$) in the $NaNO_2$ group compared with the control group. $NaNO_2$ significantly increased the testis's weight as well as the gonad somatic index ($p < 0.05$). The OC+ $NaNO_2$ group significantly reduced testicular weights and gonad somatic index and increased body weight returning them near control values ($p < 0.05$) (Table 2).

Table 1. Primers and reaction parameters.

Gene	Sequence	Annealing temp.	Product size	Reference
B-actin-	F-gctgagtctcccttggaact R-gtacctacacccacagcact	55°C	119 bp	Matuq Al-Yasi *et al*. (2021)
TNF-α	F-ctcggcctcttctcattcct R-tggacctgatgagagggagc	55°C	124 bp	Accession number NHQ201305
P450scc	F-accccatctctgtgaccttg R-tcgacccatggcatagctag	55°C	110 bp	Matuq Al-Yasi *et al*. (2021)
STAR	F-cgtggctgctcagtattgac R-agtccttaacactgggcctc	55°C	145 bp	Matuq Al-Yasi *et al*. (2021)

Abbreviations: β-actin: Beta-actin; TNF-α: Tumor necrosis factor alpha; StAR: Steroidogenic acute regulatory protein; P450scc: Cytochrome P450 Family 11 Subfamily A, Member 1.

Sperm characteristics

Our findings listed in Table 3, showed that compared to the control group, the total and progressive motility of sperm were significantly reduced ($p < 0.05$) when exposed to $NaNO_2$. It also had a significant negative impact on the sperm's plasma membrane integrity and acrosomal integrity, as well as its viability, in addition, to significantly increasing abnormal sperm morphology. The OC showed a noticeable rise in sperm's plasma membrane integrity as well as a significant decline in sperm abnormal morphology in contrast to the $NaNO_2$ at ($p < 0.05$). $NaNO_2$ + OC revealed notable amelioration in total motility, progressive motility, plasma membrane integrity, acrosomal integrity, and viability, in addition to a substantial decrease in abnormal morphology as contrasted with the $NaNO_2$ group ($p < 0.05$).

Oxidative stress markers

In Table 4, $NaNO_2$ resulted in a significant elevation in MDA levels and a notable decrease in SOD activity compared to both the control and OC group, our findings of $NaNO_2$ were reversed in the $NaNO_2$ + OC group at ($p < 0.05$).

Hormonal analysis

In Table 5, serum testosterone was significantly decreased in response to $NaNO_2$ toxicity in contrast to the control; this impact was significantly neutralized in the $NaNO_2$ + OC group. $NaNO_2$-intoxicated rats' group exhibited a notable increase in serum FSH and LH levels, these increases were restored with concurrent administration of $NaNO_2$ + OC. All results of hormonal analysis were significantly different at $p < 0.05$.

TNF-α, StAR, and cytochrome P450scc levels in the testicular tissue

As shown in Figure 1, all results of the gene expression analysis were significantly different at ($p < 0.05$). There was a significant increase in TNF-α levels and a significant decrease in P450scc (cholesterol side-chain cleavage) and StAR (Steroidogenic Acute Regulatory protein) levels in the $NaNO_2$ group compared to all other groups.

Table 2. The weight of the body and testicles, in addition to the gonad somatic index.

Parameters	Groups			
	Control	$NaNO_2$	OC	$NaNO_2$ + OC
Final Body weight (g)	290.5 ± 7.9[a]	237.2 ± 5.38[b]	277.4 ± 7.48[a]	273.7 ± 7.65[a]
Testis weight (g)	1.47 ± 0.06[a]	1.92 ± 0.07[b]	1.44 ± 0.05[a]	1.5 ± 0.04[a]
Gonadosomatic index	0.52 ± 0.03[a]	0.82 ± 0.04[b]	0.52 ± 0.03[a]	0.56 ± 0.02[a]

Values are presented as the Mean ± SEM. Different superscripts denote significant differences between groups at $p < 0.05$. OC: *Odontonema cuspidatum* extract.

Table 3. The proportions of sperm characteristics of the six groups.

Parameters	Groups			
	Control	$NaNO_2$	OC	$NaNO_2$ + OC
Total motility (%)	47.00 ± 1.37[ab]	32.80 ± 1.28[c]	48.40±1.72[a]	41.20 ± 1.8[b]
Progressive motility (%)	43.20 ± 0.58[a]	12.00 ± 1.22[b]	44.20±1.43[a]	30.00±0.84[c]
Viability (%)	52.40 ±1.12[a]	31.60 ±1.03[b]	53.80±2.45[a]	41.40±1.69[c]
Plasma membrane integrity (%)	32.20 ± 2.8[a]	15.60 ±1.16[b]	41.60±1.17[c]	27.80±2.05[a]
Abnormal morphology (%)	8.600 ± 0.6[a]	16.20 ±0.48[b]	4.400 ± 0.5[c]	11.80±1.53[a]
Acrosomal integrity (%)	96.20±1.15[a]	81.60 ±0.74[b]	97.80±0.58[a]	91.20 ± 0.8[c]

Values are expressed as Mean ± SEM. Different superscripts denote significant differences between groups at $p < 0.05$. OC: *Odontonema cuspidatum* extract.

Table 4. Oxidative stress markers in the experimental groups.

	Groups			
parameters	Control	$NaNO_2$	OC	$NaNO_2$ + OC
Testicular SOD (U /mg protein)	7.50 ± 0.57[a]	2.005 ± 0.19[b]	9.63 ± 0.28[c]	5.435 ± 0.53[d]
Testicular MDA (nmole/mg)	1.23± 0.024[a]	2.33 ± 0.14[b]	0.82 ± 0.013[c]	1.33 ± 0.066[a]

Values are expressed as Mean ± SEM. Different superscripts denote significant differences between groups at $p < 0.05$. Abbreviations: SOD, Superoxide dismutase; MDA, malondialdehyde; OC, *Odontonema cuspidatum* extract.

Table 5. The hormonal Analysis in the experimental groups.

Parameters	Groups			
	Control	$NaNO_2$	OC	$NaNO_2$ + OC
Testosterone (pg /ml)	226.1 ± 2.1[a]	158.7 ± 3.72[b]	228.3± 1.65[a]	186.2± 1.36[c]
LH (mIU/ml)	1.94 ± 0.12[a]	2.71 ± 0.16[b]	1.94 ± 0.07[a]	2.127± 0.11[a]
FSH (IU/L)	4.453 ± 0.23[a]	6.311 ± 0.36[b]	4.54 ± 0.21[a]	5.17± 0.07[a]

Values are expressed as Mean ± SEM (standard error of the mean). different superscripts denote significant differences between groups at $p < 0.05$. Abbreviations: FSH, follicle-stimulating hormone; LH, luteinizing hormone; OC, *Odontonema cuspidatum* extract.

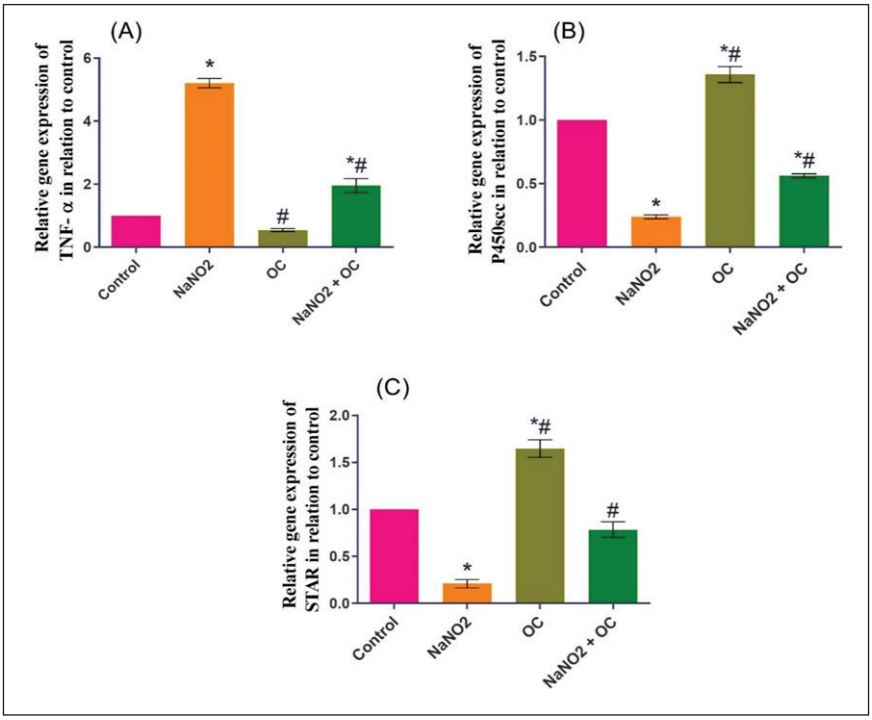

Fig. 1. Ameliorative impact OC extracts on the gene expression levels of TNF-α, StAR, and Cytochrome P450) in the testicular tissue on disturbance induced by $NaNO_2$ toxicity. The graphs represent the mean fold change ± SEM. *Significant difference as compared with the control rat groups at $p < 0.001$, # significant difference as compared with $NaNO_2$ rat group at $p < 0.001$. (A) (TNF-α), Tumor necrosis factor-alpha. (B) (StAR), Steroidogenic acute regulatory protein. (C) (P450scc), Cytochrome P450 Family 11 Subfamily A. (OC), *Odontonema cuspidatum* extract.

The group treated with $NaNO_2$ + OC exhibited significantly lower TNF-α levels and a significantly greater elevation in P450scc and StAR levels in contrast to $NaNO_2$.

Histopathological findings

The lesions of the testicular tissues are illustrated in Figure 2. The control group showed normal spermatogenic cell layers, the first layer is the primary spermatogenic cells followed by the secondary, tertiary, and spermatid layers. There was an obvious spermatogenesis associated with normal sperms within the seminiferous tubule lumen. $NaNO_2$ caused marked testicular degeneration extended along the spermatogenic layers. The spermatogenic cells within the different layers showed nuclear pyknosis, atrophy, and loss of adhesion between each other. In addition to severe edema associated with Leydig's cell hyperplasia in the interstitial tissue, in the OC group, the testicular section had normal seminiferous tubules and a noticeable increase in spermatogenesis, accompanied by an increased number of sperm within the lumen of the seminiferous tubule. The testicular section of

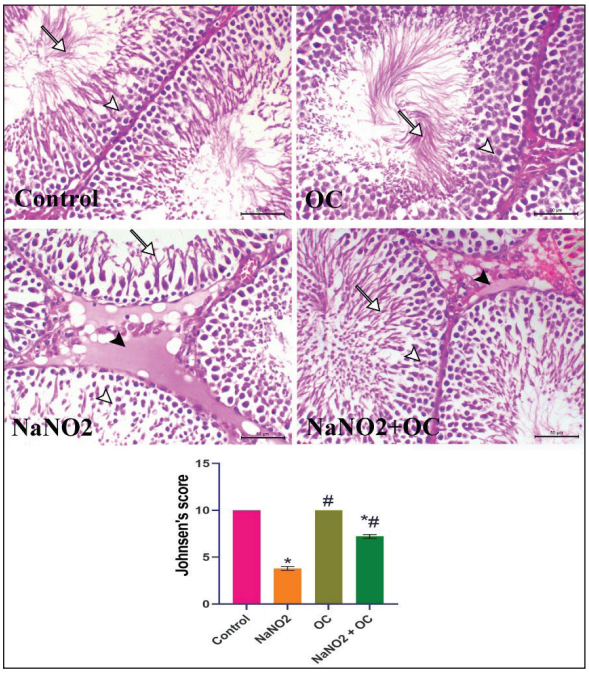

Fig. 2. Histopathological findings of the experimental groups. In the control group, the arrowhead and arrow indicate sperm within the lumen. In the $NaNO_2$ group, the white arrowhead reveals atrophic degenerated spermatogenic cells, the arrow indicates a spermatid layer, black arrowhead indicates interstitial edema. In the OC group, the white arrowhead reveals normal spermatogenic cells, the arrow indicates a spermatid layer. In the $NaNO_2$ + OC group, the white arrowhead indicates mild nuclear pyknosis of spermatogenic cells, the arrow indicates the presence of sperms within the lumen of the seminiferous tubule, and the black arrowhead shows mild to moderate interstitial edema. Scale bar = 50 µm. The graph of Johnsen's score represents the mean ± SEM. * Significant difference as compared with the control rat groups at $p < 0.001$, # Significant difference as compared with $NaNO_2$ rat group at $p < 0.001$. OC, *Odontonema cuspidatum* extract.

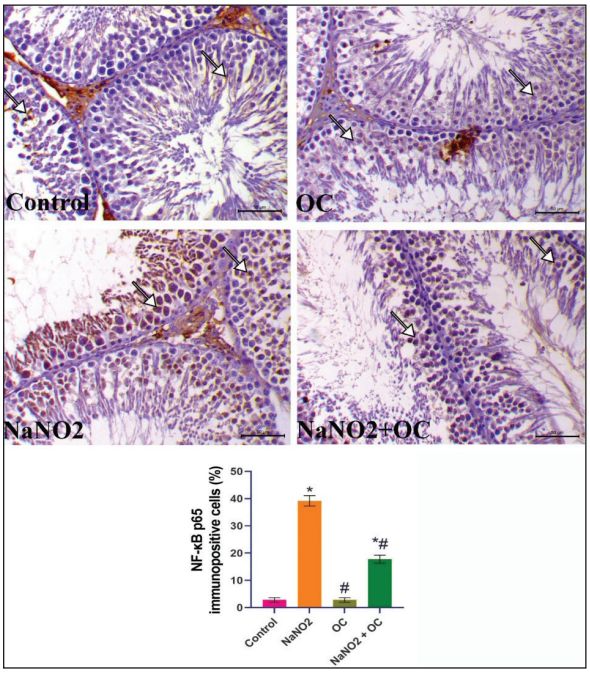

Fig. 3. The testicular sections immunostained for NF-κB p65 in the experimental groups. The arrow indicates a positive expression that markedly increases in the $NaNO_2$ group and decreases in the NaNO2 + OC group, the scale bar is set at 50 µm. The graph demonstrates the mean NF-κB p65 immunopositive cells (%) in each group represented in bars and the SEM represented in the T-shaped lines over the bars. * Significant difference as compared with the control rat groups at $p < 0.001$, # Significant difference as compared with $NaNO_2$ rat group at $p < 0.001$. Abbreviations: NF-κB p65, the nuclear factor kappa B; OC, *Odontonema cuspidatum* extract.

the $NaNO_2$ + OC group showed a marked decrease in degenerative changes compared to $NaNO_2$, mild nuclear pyknosis, mild edema in the interstitial tissue, and slight Leydig's cell hyperplasia compared to the $NaNO_2$ group According to Johnsen's score, the control and OC showed higher scores within the examined groups ($p < 0.001$), while the $NaNO_2$ showed a notable decrease in Johnsen's score. At ($p < 0.001$), the $NaNO_2$ + OC revealed a significantly higher Johnsen's score as contrasted with $NaNO_2$ ($p < 0.001$).

Immunohistochemical findings The testicular sections immunostained for NF-κB p65 were illustrated in Figure 3.

The control and OC groups showed slight NF-κB p65 immunostaining within the spermatogenic cells ($p < 0.001$). The $NaNO_2$ group showed marked NF-κB p65 immunostaining within the cytoplasm and nucleus of the spermatogenic cells ($p < 0.001$). The $NaNO_2$ + OC group showed a notable reduction in NF-κB p65 expression within the spermatogenic cells ($p < 0.001$).

In Figure 4, caspase-3 immunoexpression within the testicular tissue of the control and OC exhibited a slight expression in the spermatogenic cells' cytoplasm, while $NaNO_2$ revealed an obvious nuclear and cytoplasmic expression of the seminiferous tubule's germinal epithelium ($p < 0.001$). There was a remarkable decrease in caspase-3 immunoexpression within seminiferous tubules in the $NaNO_2$ + OC group ($p < 0.001$).

The testicular sections that were immunostained for PCNA are illustrated in Figure 5. There was a marked nuclear immunostaining within the spermatogenic lining epithelium of the control and OC groups ($p < 0.001$). $NaNO_2$ showed a marked decrease in PCNA immunostaining, which was only noticed within the primary spermatogonia ($p < 0.001$). The $NaNO_2$+ OC group showed a remarkable increase in PCNA antibodies within the germinal epithelium ($p < 0.001$).

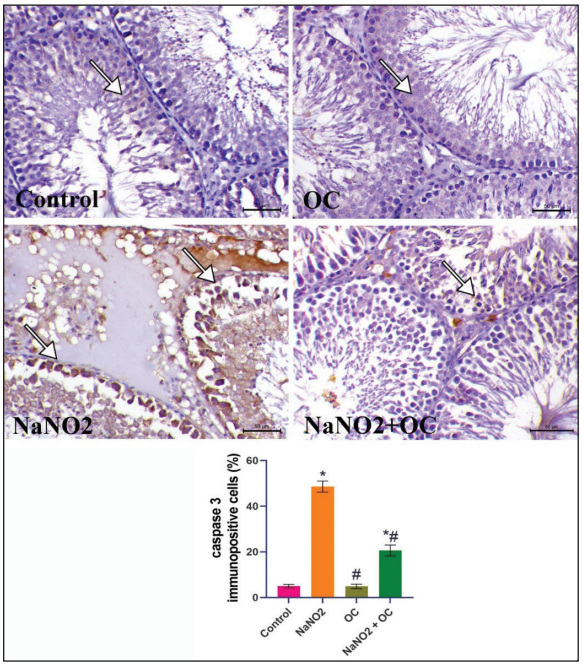

Fig. 4. The testicular sections are immunostained for caspase-3 in the experimental groups. The arrow indicates mild caspase 3 expression in the Control and OC groups. The arrow in the $NaNO_2$ group indicates marked caspase 3 immunostaining within spermatogenic cells. $NaNO_2$ + OC group is showing a decrease in caspase 3 expression indicated by arrows. Scale bar = 50 µm. The graph demonstrates the mean caspase-3immunopositive cells (%) in each group represented in bars and the SEM represented in the T-shaped lines over the bars. * Significant difference as compared with the control rat groups at $p < 0.001$, # Significant difference as compared with $NaNO_2$ rat group at $p < 0.001$. OC: *Odontonema cuspidatum* extract.

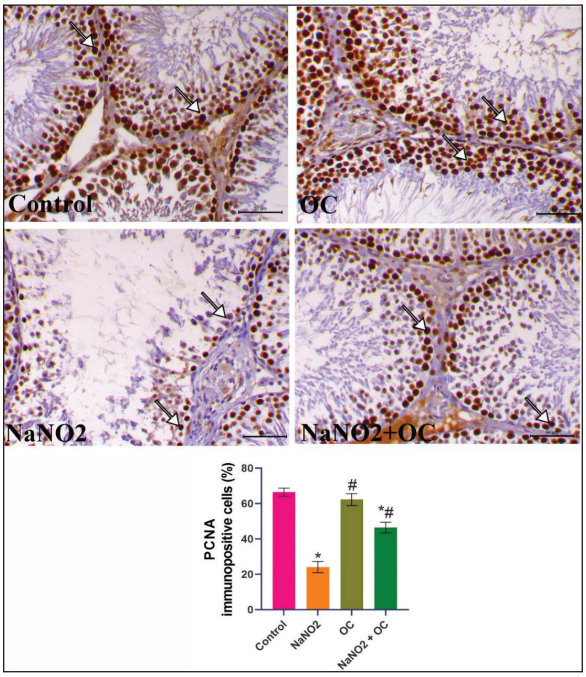

Fig. 5. The testicular sections are immunostained for PCNA in the experimental groups. The arrow indicates nuclear positive expression of PCNA antibody, scale bar = 50 µm. The graph demonstrates the mean PCNA immunopositive cells (%) in each group represented in bars and the SEM represented in the T-shaped lines over the bars. * Significant difference as compared with the control rat groups at $p < 0.001$, # Significant difference as compared with $NaNO_2$ rat group at $p < 0.001$. Abbreviations: PCNA, Proliferating cell nuclear antigen; OC, *Odontonema cuspidatum* extract.

Discussion

$NaNO_2$ is a primary preservative found in many foods, responsible for the red color of meat (Sindelar and Milkowski, 2012), and hinders the growth of *Clostridium botulinum* (Difonzo *et al*., 2022). However, it reacts with amines in the stomach resulting in the formation of nitrosamines that have harmful effects on body organs and have been linked to several types of human tumors (Hassan and Yousef, 2010).

The flavonoids of OC have an ameliorative impact against $NaNO_2$ toxicity due to their antioxidant activity; these flavonoids exert their activity as antioxidants through two mechanisms: First, the "direct mechanism" is scavenging and reduction to ROS, where the phenolic components of the flavonoid molecule transfer an electron or a hydrogen atom (Alov *et al*., 2015).

Second, the "indirect method" involves their phenolic moieties' oxidation, these oxidative compounds interact with specific proteins rather than ROS directly to increase the endogenous antioxidant capacity of cells (Erlank *et al*., 2011; Dinkova-Kostova and Talalay, 2008); therefore, the flavonoid molecule itself does not initiate the antioxidant effect; rather, a metabolite that comes from the oxidation of the flavonoid molecule does (Bolton and Dunlap, 2017).

Verbascoside was also isolated from the same plant parts (Refaey *et al*., 2017), it inhibits lipid peroxidation (Liu, 2003) due to the binding with membrane phospholipids despite being hydrophilic (Funes *et al*., 2010). In addition, it also prevents oxidation of low-density lipoproteins (Cardinali *et al*., 2012), and demonstrated activity in reducing inflammation (Paola *et al*., 2011).

Our findings indicated that administering $NaNO_2$ led to a notable reduction in final body weights which aligns with the prior research (Akintunde *et al*., 2014) that reported an age-related rise in nitrite production. According to our results, rats' testicular weight and gonadosomatic index were both increased by $NaNO_2$, and this was also consistent with Alyoussef and Al-Gayyar (2016), who reported that it could be caused by testicular anoxia or enhanced gonadotrophin due to a decrease in testosterone's inhibiting effects.

The findings of the $NaNO_2$ group revealed a noticeable decline in sperm motility, integrity of both the plasma

membrane and acrosome, and sperm viability, as well as a notable rise in abnormal sperm morphology, this might be explained by greater oxidative stress in this group since sperm's plasma membrane is composed of a large quantity of polyunsaturated fatty acids (Bansal and Bilaspuri, 2011) and scavenger enzymes are present in their cytoplasm in little amounts (Saleh and HCLD, 2002; Sharma and Agarwal, 1996), the link between ROS and reduced motility might result from the depletion of the intracellular ATP and damaged axonemal tissue and immobilizes sperm (Bansal and Bilaspuri, 2011).

Our research also revealed that administering $NaNO_2$ reduced testosterone levels, indicating a disruption in steroidogenesis, this may be attributed to lower testicular StAR gene expression, proven in our gene expression analysis, which could have a role in inhibiting the synthesis of testosterone (Mosbah *et al*., 2018), cholesterol is transmitted to the inner mitochondrial membrane by the StAR, where it is converted by P450scc into pregnenolone, which is then converted into testosterone (Miller, 2017).

We showed a marked increase in FSH and LH concentrations in the $NaNO_2$ group in contrast to the control, inadequate feedback inhibition by testosterone can be used to explain this rise in gonadotropins (Alyoussef and Al-Gayyar, 2016). On the other hand, prior studies were inconsistent with our work using different doses (Darbandi *et al*., 2018; Adelakun *et al*., 2019), body steroid levels are disturbed dose dependently by $NaNO_2$ (Kuzhiumparambil and Fu, 2013). Treatment with OC in the $NaNO_2$ + OC group significantly improved these bad impacts by getting the rats' serum back to its regular hormonal balance.

Administration of OC in the co-treated group significantly alleviated the impact of $NaNO_2$ on sperm characteristics due to the antioxidant activity of OC, concurrent with a marked decline in MDA and an increase in SOD activity.

The resulting oxidative stress is confirmed by the rise in MDA concentration, a marker for lipid peroxidation, and a distinct decrease in SOD activity in our biochemical findings (Table 5), which concurs with the previously discussed findings (Adelakun *et al*., 2019), which could be because of a concurrent rise in the production of free radicals such as H_2O_2 and OH in the $NaNO_2$ group's testes.

We expanded our research to identify what's behind the rise in oxidative stress; our results revealed that the $NaNO_2$ group significantly upregulated the expressions of the TNFα gene (pro-inflammatory cytokine), and reduced StAR and P450scc genetic expressions, the increase in pro-inflammatory cytokine levels can be due to cell peroxidation by $NaNO_2$.

This elevated TNFα level in the $NaNO_2$ group damages spermatogenesis. $NaNO_2$ + OC demonstrated a substantial drop in TNFα, confirming OC's anti-inflammatory properties. The flavonoid part of OC also inhibits pro-inflammatory enzymes such as cyclooxygenase-2 and lipoxygenase and activates mitogen-activated protein kinase and protein kinase C (Santangelo *et al*., 2007). These effects were reversed when OC was administered in combination with $NaNO_2$.

The histopathological results of the $NaNO_2$ group revealed interstitial edema in the testes, leading to increased testicular weight, which is induced by tissue anoxia and hemic ischemia, accompanied by atrophy to germinal epithelium and arrest of spermatogenesis. The co-treatment in the OC+ $NaNO_2$ group decreased testicular edema and so significantly decreased testicular weights in addition to lowering the gonadosomatic index, returning them to near-average weights similar to the control group. In addition, our histological findings indicate the presence of Leydig's cell hyperplasia, this hyperplasia is only to compensate for the decreased testosterone (Mylchreest *et al*., 2002), the decline in testosterone concentration is not reversed, it is the main androgenic hormone which is essential for secondary sexual characteristics, spermatogenesis, and sperm cell maturation, producing substantial fertility problems can be caused by a testosterone synthesis (Mohamed *et al*., 2017).

NF-κB P65 controls the gene transcription of inflammatory mediators and is essential for controlling inflammation (Ren *et al*., 2019), NF-κB P65 presents in the cytoplasm of healthy cells in the form of dimer comprising the protein subunits p50/p65 and its inhibitor (IkB), nevertheless, if the cell is exposed to oxidative damage, such as $NaNO_2$, this dimerization is disrupted, and IkB degraded in the proteasome (Doshi *et al*., 2012). IkB degradation enables NF-κB P65 to enter quickly the nucleus and then attach to DNA to control the inflammation (Zhang and Sun, 2015), including TNFα (Zhao *et al*., 2017). We observed marked immunostaining of NF-κB P65 within the cytoplasm and nucleus of spermatogenic cells that indicated testicular inflammation which was reversed in the $NaNO_2$ + OC treated group.

Caspase-3 immunostaining in the testicular tissues that received $NaNO_2$ is notably increased and is regarded as the apoptosis' last executor (Kumar *et al*., 2020). In considering this, it is crucial to remember that the increased oxidative stress induced by $NaNO_2$ causes DNA damage, ultimately resulting in apoptosis (Sherif and Al-Gayyar, 2013).

The equilibrium between germ cell proliferation, survival, and apoptosis is known to be necessary for successful spermatogenesis, and disruptions in the control of any of these may cause spermatogenesis to fail (Tan *et al*., 2007; Richburg, 2000).

PCNA is expressed in proliferating spermatogonia and spermatocytes and is an indicator of cellular proliferation (Tousson *et al*., 2011). As so, immunocytochemical analysis of PCNA is a useful indicator for assessing testicular germ proliferation. We observed a significant reduction in PCNA immunostaining expression in the NaNO2 group's testes, while the $NaNO_2$ + OC group revealed an increase in PCNA in addition to lowering caspase immunoreactive cells.

Conclusion

Our study shows evidence that *OC* extract ameliorates testicular damage induced by $NaNO_2$ by preventing oxidative stress, improving sperm parameters, and returning the proper balance of inflammatory cytokines.

Author contributions

Nesma H. Elsawy: writing, interpretation. Samir A. Elshazly and Azza M. Elkattawy: experiment design. Khaled A. Kahilo and Nasr E. Nasr: revision, editing. Mohamed S. Refaey: extract preparation. Mona Assas and Aml S. hashem: writing the manuscript. Essam A Almadaly: methodology, editing. Walied Abdo: histopathology, immunohistochemistry. Doaa Abdullah Dorghamm and Tarek K. Abouzed: data analysis. The completed version of this work was approved by all contributors.

Conflict of interest

All authors declare that there is no conflict of interest.

Funding

This work did not get any funding.

Data availability

All data are provided in the manuscript.

References

Adelakun, S.A., Ukwenya, V.O., Ogunlade, B.S., Aniah, J.A. and Ibiayo, A.G. 2019. Nitrite-induced testicular toxicity in rats: therapeutic potential of walnut oil. Jbra Assist. Reprod. 23, 15.

Akhzari, M., Shafiee, S.M., Rashno, S. and Akmali, M. 2019. Berberine attenuated oxidative stress induced by sodium nitrite in rat liver. Jundishapur J. Nat. Pharm. Prod. 14(1), e68532.

Akintunde, O., Adenowo, T. and Kehinde, B. 2014. Some adverse effects of nitrite on oxidative status and histological structures of adult male wistar rats testes. Amer. J. Res. Commun. 2, 227–241.

Almadaly, E., El-Kon, I., Heleil, B., Fattouh, E.-S., Mukoujima, K., Ueda, T., Hoshino, Y., Takasu, M. and Murase, T. 2012. Methodological factors affecting the results of staining frozen–thawed fertile and subfertile japanese black bull spermatozoa for acrosomal status. Anim. Reprod. Sci. 136, 23–32.

Almadaly, E.A., Farrag, F.A., Saadeldin, I.M., El-Magd, M.A. and Abd El-Razek, I.M. 2016. Relationship between total protein concentration of seminal plasma and sperm characteristics of highly fertile, fertile and subfertile barki ram semen collected by electroejaculation. Small Rumin. Res. 144, 90–99.

Alov, P., Tsakovska, I. and Pajeva, I. 2015. Computational studies of free radical-scavenging properties of phenolic compounds. Curr. Topics Med. Chem. 15, 85–104.

Aly, H.A. and Azhar, A.S. 2013. Methoxychlor induced biochemical alterations and disruption of spermatogenesis in adult rats. Reprod. Toxicol. 40, 8–15.

Alyoussef, A. and Al-Gayyar, M.M. 2016. Thymoquinone ameliorated elevated inflammatory cytokines in testicular tissue and sex hormones imbalance induced by oral chronic toxicity with sodium nitrite. Cytokine 83, 64–74.

Alyoussef, A. and Al-Gayyar, M. 2016. Thymoquinone ameliorates testicular tissue inflammation induced by chronic administration of oral sodium nitrite. Andrologia 48, 501–508.

Ansari, F.A., Ali, S.N., Arif, H., Khan, A.A. and Mahmood, R. 2017. Acute oral dose of sodium nitrite induces redox imbalance, dna damage, metabolic and histological changes in rat intestine. Plos One 12, E0175196.

Bancroft, J.D., Layton, C. and Suvarna, S.K. 2013. Bancroft's theory and practice of histological techniques, Churchill Livingstone Elsevier, London, UK.

Bansal, A.K. and Bilaspuri, G. 2011. Impacts of oxidative stress and antioxidants on semen functions. Vet. Med. Inter. 2011, 686137.

Bolton, J.L. and Dunlap, T. 2017. Formation and biological targets of quinones: cytotoxic versus cytoprotective effects. Chem. Res. Toxicol. 30, 13–37.

Cardinali, A., Pati, S., Minervini, F., D'antuono, I., Linsalata, V. and Lattanzio, V. 2012. Verbascoside, isoverbascoside, and their derivatives recovered from olive mill wastewater as possible food antioxidants. J. Agricul. Food Chem. 60, 1822–1829.

Chaughule, R.S. and Barve, R.S. 2023. Role of herbal medicines in the treatment of infectious diseases. Vegetos 1–11.

Darbandi, M., Darbandi, S., Agarwal, A., Sengupta, P., Durairajanayagam, D., Henkel, R. and Sadeghi, M.R. 2018. Reactive oxygen species and male reproductive hormones. Reprod. Biol. Endocrinol. 16, 1–14.

Deng, H. 2006. Nitrite anions induce nitrosative deamination of peptides and proteins. Rapid Commun. Mass Spectrometr. 20, 3634–3638.

Difonzo, G., Totaro, M.P., Caponio, F., Pasqualone, A. and Summo, C. 2022. Olive leaf extract (ole) addition as tool to reduce nitrate and nitrite in ripened sausages. Foods 11, 451.

Dinkova-Kostova, A.T. and Talalay, P. 2008. Direct and indirect antioxidant properties of inducers of cytoprotective proteins. Mol. Nutr. Food Res. 52, S128–S138.

Doshi, S.B., Khullar, K., Sharma, R.K. and Agarwal, A. 2012. Role of reactive nitrogen species in male infertility. Reprod. Biol. Endocrinol. 10, 1–11.

Erlank, H., Elmann, A., Kohen, R. and Kanner, J. 2011. Polyphenols activate nrf2 in astrocytes via h2o2, semiquinones, and quinones. Free Rad. Biol. Med. 51, 2319–2327.

Farías, J.G., Bustos-Obregón, E. and Reyes, J.G. 2005. Increase in testicular temperature and vascularization induced by hypobaric hypoxia in rats. J. Androl. 26, 693–697.

Funes, L., Laporta, O., Cerdán-Calero, M. and Micol, V. 2010. Effects of verbascoside, a phenylpropanoid

glycoside from lemon verbena, on phospholipid model membranes. Chem. Phys. Lipids 163, 190–199.
Hassan, H.A. and Yousef, M.I. 2010. Ameliorating effect of chicory (cichorium intybus l.)-supplemented diet against nitrosamine precursors-induced liver injury and oxidative stress in male rats. Food Chem. Toxicol. 48, 2163–2169.
Jensen, F.B. 2007. Nitric oxide formation from nitrite in zebrafish. J. Exper. Biol. 210, 3387–3394.
Johnsen, S.G. 1970. Testicular biopsy score count–a method for registration of spermatogenesis in human testes: normal values and results in 335 hypogonadal males. Hormone Res. Paediar. 1, 2–25.
Jørgenandmarianne, N. 2011. Use of sodium nitrite in salt-curing of atlantic salmon (salmo salar l.)–impact on product quality. Food Chem. 124, 759–766.
Kasali, F.M., Kadima, J.N., Tusiimire, J., Ajayi, C.O. and Agaba, A.G. 2022. Effects of the oral administration of aqueous and methanolic leaf extracts of chenopodium ambrosioides l.(amaranthaceae) on blood glucose levels in Wistar Rats. J. Exper. Pharmacol. 139–148.
Khalil, R., Shata, A., Abd El-Kader, E.M., Sharaf, H., Abdo, W.S., Amin, N.A. and Saber, S. 2020. Vildagliptin, a dpp-4 inhibitor, attenuates carbon tetrachloride-induced liver fibrosis by targeting erk1/2, p38α, and nf-κb signaling. Toxicol. Appl. Pharmacol. 407, 115246.
Khodjaeva, U., Bojňanská, T., Vietoris, V., Sytar, O. and Singh, R. 2013. About food additives as important part of functional food. J. Microbiol. Biotechnol. Food Sci. 2, 2125–2135.
Kozisek, F. 2007. Influence of nitrate levels in drinking water on urological malignancies: a community-based cohort study. Bju Inter. 99, 1550–1551.
Kumar, J., Haldar, C. and Verma, R. 2020. Fluoride compromises testicular redox sensor, gap junction protein, and metabolic status: amelioration by melatonin. Biol. Trace Elem. Res. 196, 552–564.
Kuzhiumparambil, U. and Fu, S. 2013. Effect of oxidizing adulterants on human urinary steroid profiles. Steroids 78, 288–296.
Liu, R.H. 2003. Health benefits of fruit and vegetables are from additive and synergistic combinations of phytochemicals. Amer J. Clin. Nutr. 78, 517s–520s.
Matuq Al-Yasi, H., El-Shazly, S.A., Ahmed, E.F., Hasan Alamer, K., Hessini, K.Y., Attia, H.A., Alkafafy, M.E., Mohamed, A.A. and Hassan, F.A. 2021. Protective effects of taif rosewater against testicular impairment induced by lead intoxication in rats. Andrologia 53, E14045.
Miller, W.L. 2017. Steroidogenesis: unanswered questions. Trend Endocrinol. Metab. 28, 771–793.
Mohamed, A.A.-R., Mohamed, W.A. and Khater, S.I. 2017. Imidacloprid induces various toxicological effects related to the expression of 3β-hsd, nr5a1, and ogg1 genes in mature and immature rats. Environ. Pollut. 221, 15–25.
Mortimer, D. and Mortimer, S. 1992. Methods of sperm preparation for assisted reproduction. Ann. Acad, Med., Singapore 21, 517–524.
Mosbah, R., Djerrou, Z. and Mantovani, A. 2018. Protective effect of nigella sativa oil against acetamiprid induced reproductive toxicity in male rats. Drug Chem. Toxicol. 41, 206–212.
Mostafa-Hedeab, G., Behairy, A., Abd-Elhakim, Y.M., Mohamed, A.A.-R., Noreldin, A.E., Dahran, N., Gaber, R.A., Alqahtani, L.S., Essawi, W.M. and Eskandrani, A.A. 2023. Green synthesized zinc oxide nanoparticles using moringa olifera ethanolic extract lessens acrylamide-induced testicular damage, apoptosis, and steroidogenesis-related gene dysregulation in adult rats. Antioxidants 12, 361.
Mylchreest, E., Sar, M., Wallace, D.G. and Foster, P.M. 2002. Fetal testosterone insufficiency and abnormal proliferation of leydig cells and gonocytes in rats exposed to di (n-butyl) phthalate. Reprod. Toxicol. 16, 19–28.
Naik, S.R., Pilgaonkar, V.W. and Panda, V.S. 2006. Evaluation of antioxidant activity of ginkgo biloba phytosomes in rat brain. Phytother. Res. 20, 1013–1016.
Nishikimi, M. 1975. Oxidation of ascorbic acid with superoxide anion generated by the xanthine-xanthine oxidase system. Biochem. Biophys. Res. Commun. 63, 463–468.
Ohkawa, H., Ohishi, N. and Yagi, K. 1979. Assay for lipid peroxides in animal tissues by thiobarbituric acid reaction. Anal. Biochem. 95, 351–358.
Oyagbemi, A. and Odetola, A. 2010. Hepatoprotective effects of ethanolic extract of cnidoscolus aconitifolius on paracetamol-induced hepatic damage in rats. Pak. J. Biol. Sci. 13, 164–169.
Paola, R.D., Oteri, G., Mazzon, E., Crisafulli, C., Galuppo, M., Toso, R.D., Pressi, G., Cordasco, G. and Cuzzocrea, S. 2011. Effects of verbascoside, biotechnologically purified by syringa vulgaris plant cell cultures, in a rodent model of periodontitis. J. Pharm. Pharmacol. 63, 707–717.
Pavlova, E., Dimova, D., Petrova, E., Gluhcheva, Y. and Atanassova, N. 2017. Comparative evaluation of the effect of sodium nitrite on reproductive organ weights and sperm count in rats and mice. Acta Morphologica Et Anthropologica 24, 10–14.
Pierre, L.L. and Moses, M.N. 2015. Isolation and characterisation of stigmasterol And B-Sitosterol from Odontonema Strictum (Acanthaceae). J. Innov. Pharm. Biol. Sci. 2, 88–95.
Pluta, R.M., Dejam, A., Grimes, G., Gladwin, M.T. and Oldfield, E.H. 2005. Nitrite infusions to prevent delayed cerebral vasospasm in a primate model of subarachnoid hemorrhage. JAMA 293, 1477–1484.
Refaey, M., Hassanein, A.M., Mostafa, M.A., Wanas, A.S. and Ali, A. 2017. Two new iridoid

glycosides from odontonema cuspidatum and their bioactivities. Phytochem. Lett. 22, 27–32.
Refaey, M., Mustafa, M., Mohamed, A. and Ali, A. 2015. Hepatoprotective and antioxidant activity of odontonema cuspidatum (nees) kuntze against ccl4-induced hepatic injury in rats. J. Pharm. Phytochem. 4, 89–96.
Ren, Z., He, H., Zuo, Z., Xu, Z., Wei, Z. and Deng, J. 2019. The role of different sirt1-mediated signaling pathways in toxic injury. Cell. Mol. Biol. Lett. 24, 1–10.
Richburg, J.H. 2000. The relevance of spontaneous-and chemically-induced alterations in testicular germ cell apoptosis to toxicology. Toxicol. Lett. 112, 79–86.
Saleh, R.A. and Hcld, A.A. 2002. Oxidative stress and male infertility: from research bench to clinical practice. J. Androl. 23, 737–752.
Santangelo, C., Varì, R., Scazzocchio, B., Di Benedetto, R., Filesi, C. and Masella, R. 2007. Polyphenols, intracellular signalling and inflammation. Annali-Istituto Superiore Di Sanita 43, 394.
Sharma, R.K. and Agarwal, A. 1996. Role of reactive oxygen species in male infertility. Urology 48, 835–850.
Sherif, I.O. and Al-Gayyar, M.M. 2013. Antioxidant, anti-inflammatory and hepatoprotective effects of silymarin on hepatic dysfunction induced by sodium nitrite. Europ. Cytokine Network 24, 114–121.
Sindelar, J.J. and Milkowski, A.L. 2012. Human safety controversies surrounding nitrate and nitrite in the diet. Nitric Oxide 26, 259–266.
Talebi, A.R., Khalili, M.A. and Hossaini, A. 2007. Assessment of nuclear dna integrity of epididymal spermatozoa following experimental chronic spinal cord injury in the rat. Inter. J. Androl. 30, 163–169.
Tan, D.X., Manchester, L.C., Terron, M.P., Flores, L.J. and Reiter, R.J. 2007. One molecule, many derivatives: a never-ending interaction of melatonin with reactive oxygen and nitrogen species? J. Pineal Res. 42, 28–42.
Tousson, E., Ali, E.M., Ibrahim, W. and Mansour, M.A. 2011. Proliferating Cell nuclear antigen as a molecular biomarker for spermatogenesis in ptu-induced hypothyroidism of rats. Reprod. Sci. 18, 679–686.
Veilleux-Lemieux, D., Castel, A., Carrier, D., Beaudry, F. and Vachon, P. 2013. Pharmacokinetics of ketamine and xylazine in young and old Sprague–Dawley Rats. J. Amer. Assoc. Lab. Anim. Sci. 52, 567–570.
Wang, W., Zhang, Z., Liu, X., Cao, X., Wang, L., Ding, Y. and Zhou, X. 2022. An improved gc-ms method for malondialdehyde (mda) detection: avoiding the effects of nitrite in foods. Foods 11, 1176.
Wu, L., Zhang, C., Long, Y., Chen, Q., Zhang, W. and Liu, G. 2022. Food additives: from functions to analytical methods. Crit. Rev. Food Sci. Nutr. 62, 8497–8517.
Zhang, H. and Sun, S.-C. 2015. Nf-Kb in inflammation and renal diseases. Cell Biosci., 5, 1–12.
Zhao, L., Liu, H., Yue, L., Zhang, J., Li, X., Wang, B., Lin, Y. and Qu, Y. 2017. Melatonin attenuates early brain injury via the melatonin receptor/sirt1/nf-κb signaling pathway following subarachnoid hemorrhage in mice. Mol. Neurobiol. 54, 1612–1621.